Particle and Fibre Toxicology

RESEARCH

Open Access

Copper oxide nanoparticles exacerbate chronic obstructive pulmonary disease by activating the TXNIP-NLRP3 signaling pathway

Woong-Il Kim[1†], So-Won Pak[1†], Se-Jin Lee[1], Sin-Hyang Park[1], Je-Oh Lim[2], Dong-il Kim[1], In-Sik Shin[1], Sung-Hwan Kim[3*] and Jong-Choon Kim[1*]

Abstract

Background Although copper oxide nanoparticles (CuONPs) offer certain benefits to humans, they can be toxic to organs and exacerbate underlying diseases upon exposure. Chronic obstructive pulmonary disease (COPD), induced by smoking, can worsen with exposure to various harmful particles. However, the specific impact of CuONPs on COPD and the underlying mechanisms remain unknown. In this study, we investigated the toxic effects of CuONPs on the respiratory tract, the pathophysiology of CuONPs exposure-induced COPD, and the mechanism of CuONPs toxicity, focusing on thioredoxin-interacting protein (TXNIP) signaling using a cigarette smoke condensate (CSC)-induced COPD model.

Results In the toxicity study, CuONPs exposure induced an inflammatory response in the respiratory tract, including inflammatory cell infiltration, cytokine production, and mucus secretion, which were accompanied by increased TXNIP, NOD-like receptor protein 3 (NLRP3), caspase-1, and interleukin (IL)-1β. In the COPD model, CuONPs exposure induced the elevation of various indexes related to COPD, as well as increased TXNIP expression. Additionally, TNXIP-knockout (KO) mice showed a significantly decreased expression of NLRP3, caspase-1, and IL-1β and inflammatory responses in CuONPs-exposed COPD mice. These results were consistent with the results of an in vitro experiment using H292 cells. By contrast, TNXIP-overexpressed mice had a markedly increased expression of NLRP3, caspase-1, and IL-1β and inflammatory responses in CuONPs-exposed COPD mice.

Conclusions We elucidated the exacerbating effect of CuONPs exposure on the respiratory tract with underlying COPD, as well as related signaling transduction via TXNIP regulation. CuONPs exposure significantly increased inflammatory responses in the respiratory tract, which was correlated with elevated TXNIP-NLRP3 signaling.

[†]Woong-Il Kim and So-Won Pak contributed equally to this work.

*Correspondence:
Sung-Hwan Kim
sunghwan.kim@kitox.re.kr
Jong-Choon Kim
toxkim@jnu.ac.kr

Full list of author information is available at the end of the article

Keywords Copper oxide nanoparticles, Chronic obstructive pulmonary disease, Thioredoxin-interacting protein, NOD-like receptor protein 3, Inflammation

Background

Industrial technology using copper oxide nanoparticles (CuONPs) has been developed over recent decades, driven by their remarkable physicochemical properties, including high surface-to-volume ratio, tiny size, and flexible functionalization [1, 2]. The application of CuONPs is gradually expanding to fields such as drug delivery, fertilizer and pesticide, and electrical engineering [3–5]. There are growing concerns about the toxic effects of CuONPs on human health, particularly industrial workers and consumers, as the increased CuONPs use increases human exposure to the particles. Exposure to CuONPs mostly occurs through inhalation; hence, various hazard assessments of inhalation exposure to CuONPs are in progress [6, 7]. Recently, inhalation exposure to CuONPs has been demonstrated to cause respiratory toxicity by producing excessive reactive oxygen species (ROS), leading to oxidative stress [2]. However, there is currently insufficient research on the exact mechanism of respiratory toxicity caused by CuONPs exposure. Particularly, the research on the effects of underlying respiratory disease is also very scarce. Furthermore, no studies investigated the mechanism responsible for the exacerbation of underlying respiratory diseases, such as chronic obstructive pulmonary disease (COPD).

COPD is characterized by narrowing of the airways and a resulting decrease in airflow. It causes dyspnea, coughing, and sputum and is linked to chronic inflammation of the lungs and airways [8, 9]. In addition to fumes and particulate matter, cigarette smoke (CS) is the primary cause of COPD [10]. CS contains various hazardous substances, including toxic chemicals, free radicals, and heavy metals [10]. Exposure to these substances causes abundant inflammatory cell infiltration of the lung tissue, leading to oxidative stress and inflammation, which can eventually result in lung failure [11]. These clinical signs of COPD can also be worsened by bacteria, fungi, and viruses [12]. Additionally, particulate matter can exacerbate COPD [13, 14], but the relationship between CuONPs and COPD remains largely unexplored, necessitating further research in this area.

Thioredoxin-interacting protein (TXNIP) is associated with apoptosis, inflammation, immunological response, proliferation, and aging, and is involved in the pathophysiology of many disorders [15–17]. Several studies showed that in a context of oxidative stress, TXNIP released by oxidized thioredoxin (TRX) binds to the NOD-like receptor protein 3 (NLRP3) inflammasome to activate and release interleukin (IL)-1β and IL-18, thereby eliciting an inflammatory response [18–20]. Mahalanobish et al. [11] reported that the TXNIP/NLRP3 pathway is activated by increasing ROS and inducing endoplasmic reticulum stress in mice exposed to cigarette smoke. Additionally, Lim et al. [21] reported that TXNIP is activated by the administration of nanomaterials. Therefore, TXNIP is expected to have a notable impact on the development of COPD as well as on nanomaterial toxicity. However, there is currently uncertainty regarding the connection between CuONPs and TXNIP-mediated inflammation in COPD. Therefore, further studies are required to comprehend the inflammatory mechanism induced by TXNIP and the pathophysiology of CuONPs-induced COPD exacerbation.

This study aimed to determine the mechanism by which CuONPs exposure exacerbates COPD by measuring inflammatory markers and performing histopathological analysis to examine the impact of CuONPs on COPD. Additionally, we explored the fundamental mechanism of the inflammatory response by focusing on the TXNIP signaling pathway and verified the changes in CuONPs-related inflammatory response when TXNIP is overexpressed or deleted.

Material & methods

Preparation of copper oxide nanoparticles

CuONPs (sized < 50 nm) were acquired from Sigma-Aldrich (St Louis, MO, USA). Prior to instillation, CuONPs were combined with phosphate-buffered saline (PBS) and ultrasonically processed for 3 min. CuONPs (0.5 mg/kg) doses were computed based on the body weight of each mouse immediately before administration.

Transmission electron microscopy (TEM; JEM-2100 F, JEOL, Tokyo, Japan) and scanning electron microscopy (SEM; Zeiss Gemini500, Carl Zeiss Meditec AG, Jena, Germany) were used to assess the morphology and primary size of CuONPs at accelerating voltages of 150 kV and 15 kV, respectively. The purity of CuONPs was determined by energy-dispersive X-ray spectroscopy (Zeiss Genini500 SEM equipped with X-max^N 150-mm^2 silicon drift detector; Oxford Instrument, Abingdon, UK). The hydrodynamic size and zeta potential of CuONPs were established by particle size and zeta potential analyzer (ELSZeno, Otsuka Electronics, Tokyo, Japan).

Animal and experimental design

Specific pathogen-free C57BL/6 mice (male, 6 weeks) were obtained from Samtako Co. (Osan, Republic of Korea). Male mice were chosen to ensure consistency in results by minimizing variability due to hormonal

fluctuations and to facilitate comparisons with previous studies on COPD in our laboratory [10, 22, 23]. The animals were kept in a setting with a relative humidity of 50±5%, an artificial 12-hour light/dark cycle, and 13–18 air changes per hour at a temperature of 22±2℃ with a standard rodent diet and water *ad libitum*. All procedures were performed according to the NIH Guidelines for the Care and Use of Laboratory Animals and approved by the Institutional Animal Care and Use Committee of Chonnam National University (CNU IACUC-YB-2021-146). The mice were divided into 5 groups (n=6) to evaluate the respiratory toxicity of CuONPs: normal control (NC) group and 4 CuONPs-treated (0.1, 0.2, 0.4, and 1.0 mg/kg) groups. On days 1, 3, and 5, CuONPs-treated groups received the CuONPs (0.1, 0.2, 0.4, and 1.0 mg/kg doses in 50 μL of PBS) via intranasal instillation under slight anesthesia using isoflurane (Isotory®, Troikaa Pharmaceuticals Ltd., Gujarat, India) and NC group received PBS (50 μL/mouse) in the same way under the same conditions. CuONPs were combined with PBS and sonicated in an ultrasonicator (SD-251 H, Sungdong Ultrasonic Co. Ltd., Seoul, Republic of Korea) for 3 min (150 W, 40 kHz) immediately before instillation (Supplementary Figure S1A).

For an experiment to explore whether CuONPs impact the exacerbation of COPD, the adapted mice were divided into 5 groups (n=6): normal control (NC) group, COPD (CSC and lipopolysaccharide (LPS) instillation) group, and 3 COPD+CuONPs (CuONPs 0.25, 0.5, and 1.0 mg/kg) groups. CSC was provided from the Korea Institute of Toxicology (Jeongeup, Republic of Korea). CSC (50 mg/kg) and LPS (0.5 mg/kg) were administered intranasally on days 1, 7, and 13 to all groups except for the NC group under slight anesthesia. On days 8, 10, and 12, CuONPs were intranasally administered to the CuONPs groups, and only vehicle was intranasally administered to the NC group and COPD group (Supplementary Figure S1B). CSC, LPS, and CuONPs doses were selected based on our preliminary experiments and previous papers [9, 10, 24].

We prepared a TXNIP overexpression model and a knockout (KO) model to determine whether TXNIP was indeed involved in the effects of CuONPs on COPD in mice. TXNIP-overexpressing mice and green fluorescent protein (GFP)-overexpressing mice as a control were established 1 week before administration of the experimental substances using the adeno-associated virus (AAV) system. TXNIP KO mice were provided by the Korea Research Institute of Bioscience and Biotechnology (Cheong-ju, Republic of Korea). C57BL/6J (wild type; WT) mice as a control were purchased from Damul Science (Daejeon, Republic of Korea). The overexpression and KO models were divided into the following 3 groups along with each control group (each group, n=6): NC, COPD, and COPD+CuONPs 0.5 mg/kg groups. The concentration of CuONPs used in this study was set at 0.5 mg/kg (equivalent to 10 μg per mouse, assuming a mouse weight of 20 g), which corresponds to a human dose of approximately 35 mg (based on a human weight of 70 kg). This dose is estimated to reflect approximately 3 weeks of exposure, based on the current National Institute for Occupational Safety and Health (NIOSH) Recommended Exposure Limit (REL) of 1 mg/m^3, assuming a breathing frequency of 15 breaths/min, a tidal volume of 600 mL/breath, and a pulmonary deposition fraction of 0.5 for 36 nm particles [25]. The procedure used in the experiment was the same as the one described in the previous paragraph (Supplementary Figure S1C and D).

DNA cloning, preparing, and purifying of AAV

We created a mouse *TXNIP* (NM_001009935.2) gene with a FLAG tag under the CAG promoter in an AAV vector utilizing Vectorbuilder's (Chicago, IL, USA) services to enable the production of TXNIP using AAV. The pAAV vector containing the target gene, pAAV2/8 (Addgene, Watertown, MA, USA), and helper plasmid pAd-DeltaF6 (Addgene) were co-transfected into 293 cells at a 1:1:1 molar ratio. The cells were collected after 3 days and lysed with AAV lysis buffer (150 Mm NaCl, 20 Mm Tris, pH 8.0). Benzonase (Sigma-Aldrich) was then added to the lysates, and centrifugation was used to eliminate the nucleic acids. In order to purify the virus, the supernatant was carefully stacked over an iodixanol gradient (15%, 25%, 40%, and 60%) in a QuickSeal tube (Hitachi, Tokyo, Japan). Then, the tube was centrifuged using the Himac CP80WX with the P90AT rotor (Hitachi) at 280,000 × g for 3 h at 14 °C. After gathering the virus from the 60% and 40% gradient interface, it was concentrated using an Amicon Ultra-15 Centrifugal Filter Unit (Sigma-Aldrich) and subjected to three washings. Lastly, the mice received an intranasal injection of either the pure AAV-TXNIP or control (AAV-GFP) viruses at a dose of 2×10^{11} viral particles per mouse.

Bronchoalveolar lavage fluid analysis

Mice were euthanized, followed by tracheotomy 2 days after the last CuONPs or CSC+LPS instillation. After left bronchus was firmly tied for histological analysis, 700 μl of sterile PBS was introduced into the lung using a tracheal cannula and then aspirated to collect bronchoalveolar lavage fluid (BALF). This process was repeated twice. The recovered BALF was centrifuged (300 × g, 10 min, 4 °C), and the supernatant was collected in fresh EP tubes to measure IL-1β, IL-6, and tumor necrosis factor (TNF)-α. Using commercial enzyme-linked immunosorbent assay kits (BD Biosciences, San Jose, CA, USA), BALF cytokine levels, including IL-1β, IL-6, and TNF-α, were assessed according to the manufacturer's procedure.

After removing the supernatant, 500 µl of PBS was newly added to the remaining pellet and dissolved. Then, the total number of BALF cells was measured with Cell Countess III Thermo Fisher Scientific, Waltham, MA, USA). The cells were adhered to the slides using a cytospin (Hanil Science Industrial Co., Ltd., Seoul, Republic of Korea) and then stained with Diff-Quik reagent (Thermo Fisher Scientific) to count inflammatory cells under a 200× magnification light microscope. The visible inflammatory cell count and the overall cell count from Cell Countess III were used to determine the differential inflammatory cell count in BALF.

Oxidative stress analysis

The expression level of 8-hydroxyl deoxyguanosine (8-OHdG; Santa Cruz Biotechnology, Dallas, TX, USA) in the lungs was measured by immunofluorescence using a confocal microscope. Malondialdehyde (MDA) level and superoxide dismutase (SOD) activity were measured using commercial kits (Cayman, Ann Arbor, MI, USA) in the supernatant obtained by homogenizing superior and postcaval lobes of each mouse lung.

Histopathology and immunohistochemistry

Histopathological examination was performed on the lung collected from the animals as previously described [26, 27]. The left lung tissue was fixed using 10% neutral buffered formalin after collecting the BALF samples. Following a 48-hour fixation period, the tissues were paraffin-embedded, sectioned at a 4-µm thickness, and stained using hematoxylin and eosin (Sigma-Aldrich) and periodic acid-Schiff solution (IMEB Inc., San Marcos, CA, USA) to assess airway inflammation and mucus production, respectively. For immunohistochemistry (IHC), the sectioned paraffin tissues were prepared as previously described [28]. The primary antibodies used to evaluate protein expression were anti-TXNIP (1:200 dilution; Novus Biologicals, Littleton, CO, USA) and anti-IL-1β (1:200 dilution; Abcam, Cambridge, UK). All quantitative analyses related to the lung tissue were conducted using an image analyzer (Image J software, version 1.51).

Western blot analysis

We conducted immunoblotting as previously described [26]. The following primary antibodies and dilutions were used: TXNIP (1:1000; Novus Biologicals), NLRP3 (1:1000; Abcam), caspase-1 (1:1000; Adipogen Life Science, Liestal, Switzerland), IL-1β (1:1000; Abcam), and β-actin (1:1000; Cell signaling Technology, Danvers, MA, USA). The following secondary antibodies and dilutions were used: goat anti-mouse immunoglobulin (Ig) G (1:10000; Thermo Fisher Scientific), and goat anti-rabbit IgG (1:10000; Thermo Fisher Scientific). Using Chemi-Doc (Bio-Rad Laboratories, Hercules, CA, USA), the relative densitometric protein value was established.

Cell culture and cell viability assay

NCI-H292 cell line derived from cervical node metastasis of pulmonary mucoepidermoid carcinoma was purchased from the American Type Culture Collection (Manassas, VA, USA). The cells were cultivated in RPMI 1640 medium (WELGENE, Gyungsan, Republic of Korea) with 10% fetal bovine serum and antibiotics, followed by incubation in a humidified chamber maintained at 37 °C with 5% CO_2. Cell viability was measured using the EZ-Cytox cell viability assay kit (Dogenbio, Seoul, Republic of Korea) as previously described [29].

mRNA expression measurement

As directed by the manufacturer, RNA was extracted using the HiGene Total RNA Prep Kit (Biofact, Daejeon, Republic of Korea). A cDNA kit (Qiagen, Hilden, Germany) was used to reverse transcribe the extracted total RNA into cDNA. The previously mentioned qRT-PCR technique was employed to measure the mRNA expression of inflammatory cytokines [29]. The quantitative analysis was conducted using the Real-Time PCR Detection System (Bio-Rad Laboratories). qRT-PCR assays were performed utilizing particular forward and reverse primers shown in Supplementary Table S1.

Immunofluorescence and confocal microscopy

Double immunofluorescence was performed according to a prior study [30]. The utilized antibodies were as follows: TXNIP (1:200; Novus Biologicals), NLRP3 (1:200; Abcam), FITC (Rabbit IgG; 1:100; Sigma-Aldrich), and TRITC antibody (Mouse IgG; 1:100; Sigma-Aldrich). Fluorescence images were captured using a confocal microscope (ZEISS, Oberkochen, Germany) at 630× magnification.

Small interfering RNA transfection

TXNIP and scrambled siRNA were transfected into NCI-H292 cells using the Lipofectamine™ RNAiMAX reagent (Invitrogen, Waltham, MA, USA) following the manufacturer's instructions. After TXNIP expression was inhibited, the cells were treated with 2 µg/mL CuONPs or free medium and were harvested after 6 h.

Statistical analysis

Data were expressed as the mean ± standard deviation. One-way ANOVA analysis of variance was used to test for statistical significance among experiment groups followed by Tukey's multiple comparisons test. P values < 0.05 indicated statistical significance.

Results

Physicochemical characteristics of CuONPs

As analyzed by SEM and TEM, CuONPs were spherical. The primary size of CuONPs was 43.96±12.36 nm (Fig. 1A). Figure 1B shows that the atomic ratio derived using energy-dispersive X-ray spectroscopy is close to 1 with Cu 45.37% and O 54.63%, indicating that the material was CuO. The ELSZeno showed the hydrodynamic size in PBS and zeta potential of 758.8±162.9 nm and −25.63 mV, respectively.

Pathophysiological alteration in CuONPs-exposed mice

Although the CuONPs 0.1 mg/kg group demonstrated an increased inflammatory cell count and cytokines production in the BALF compared to the NC group, the increase was not significant (Supplementary Figure S2A–G). However, the groups exposed to >0.2 mg/kg CuONPs had a markedly increased inflammatory cell count, including neutrophils, macrophages, and lymphocytes, in the BALF compared with the NC group, which were accompanied by the significant elevation of cytokines, including IL-1β, IL-6, and TNF-α. Additionally, CuONPs (≥0.2 mg/kg) groups exhibited inflammatory cell infiltration into bronchial and alveolar lesions and increased mucus production compared with the NC group (Supplementary Figure S2H–J). The expression of TXNIP and inflammation-related proteins markedly increased in a dose-dependent manner in CuONPs groups compared with the NC group (Fig. 2).

Pathophysiological alterations of CuONPs-treated NCI-H292 cells

The highest concentration of CuONPs used in the in vitro experiments was determined to be 2.0 μg/mL based on cell viability results, as higher concentrations led to excessive cytotoxicity (Supplementary Figure S3A). The CuONPs-treated cells showed a significantly increased mRNA expression of TNF-α, IL-1β, IL-6, and antioxidant enzymes including SOD and glutathione reductase (GR) with elevated production of IL-6 and IL-8 in a concentration-dependent manner compared with the non-treated cells (Supplementary Figure S3B–H). Furthermore, CuONPs-treated cells had a significantly increased expression of TXNIP, NLRP3, caspase-1, and IL-1β compared with non-treated cells (Fig. 3A–F). However, TXNIP siRNA counteracted the elevation of NLRP3, caspase-1, and IL-1β expression induced by CuONPs treatment (Fig. 4A–E).

Effects of CuONPs exposure on the progression of COPD mice

The COPD group exhibited significantly increased inflammatory cell counts and inflammatory cytokines of the BALF compared with the NC group (Fig. 5A–G). CuONPs exposure significantly elevated inflammatory cell counts, including neutrophils, macrophages, and lymphocytes, and inflammatory cytokines, including IL-1β, IL-6, and TNF-α, in COPD mice compared to the COPD group. These events were consistent with the

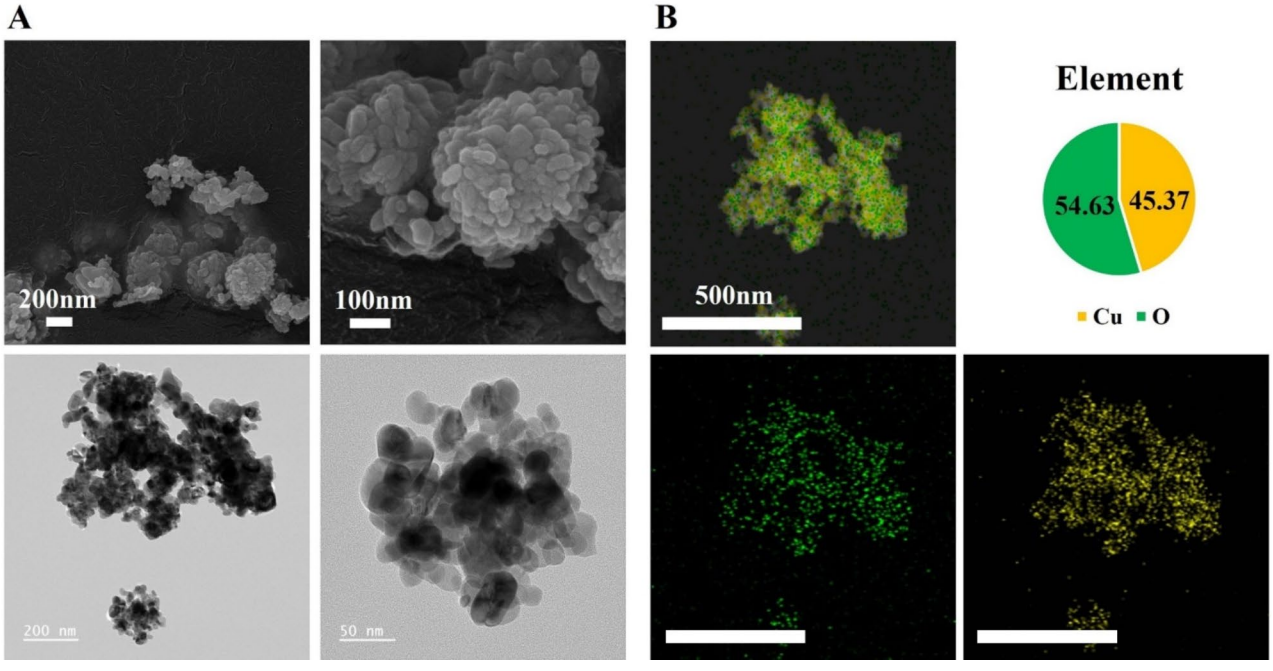

Fig. 1 Physicochemical characteristics of CuONPs. (**A**) The morphology of CuONPs was measured by scanning electric microscopy (Bar = 200 and 100 nm) and transmission electron microscopy (Bar = 200 and 50 nm). (**B**) The purity of CuONPs was measured by energy-dispersive X ray spectroscopy (Cu: 45.37%, O: 54.63%; Bar = 500 nm)

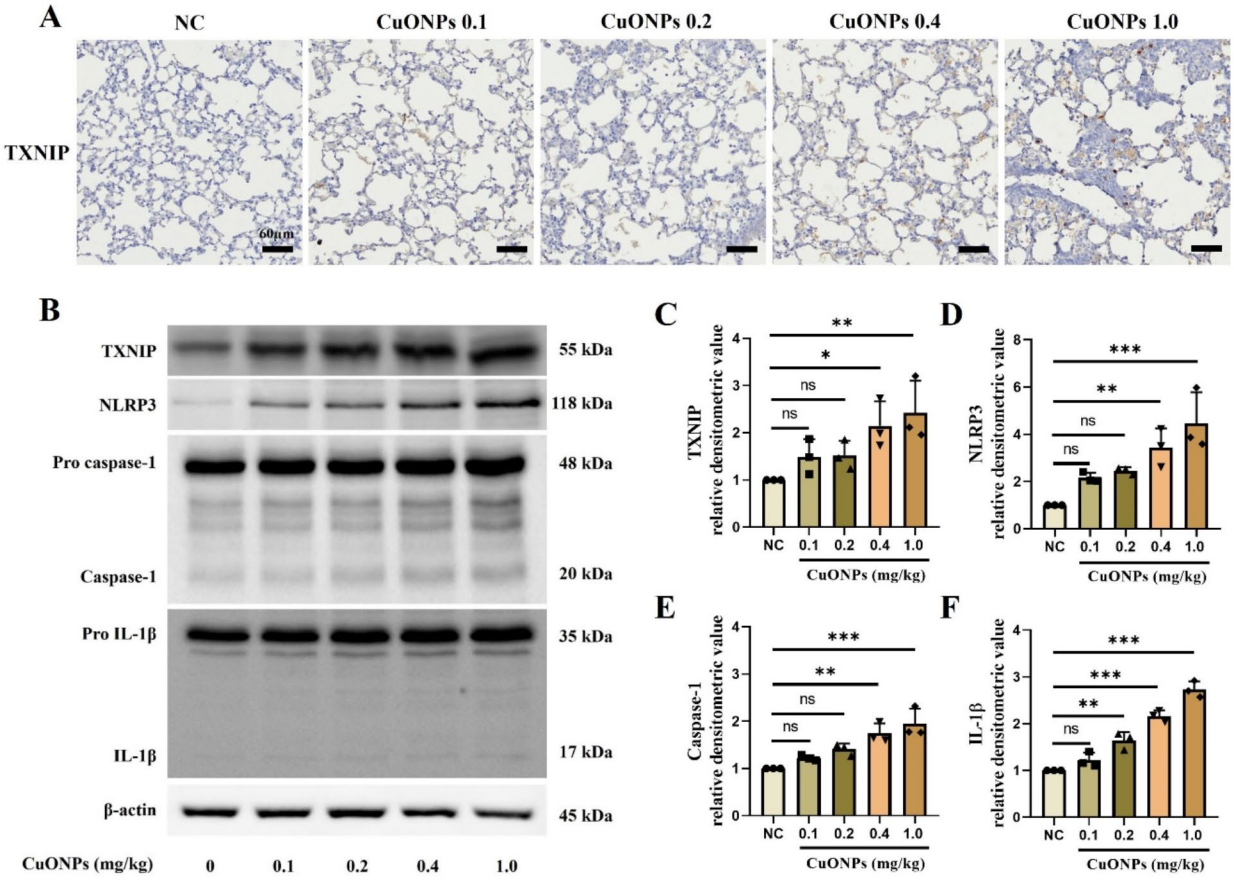

Fig. 2 Pathophysiological alteration of CuONPs-exposed mice. (**A**) Expression of TXNIP (× 200, Bar = 60 nm). (**B**–**F**) Protein expression and relative densitometric values. Data are indicated as means ± SD ($n = 3$). *, **, *** Significant differences from the NC group, $p < 0.05$, $p < 0.01$, and $p < 0.001$, respectively

results of histological analysis. CuONPs exposure significantly increased inflammatory cell infiltration and mucus production in COPD mice compared with the COPD group (Fig. 5H–J). Additionally, CuONPs exposure markedly increased 8-OHdG and MDA expression in COPD mice compared with the COPD group (Fig. 5K and M). In contrast, SOD significantly decreased in CuONPs-exposed COPD groups compared with controls (Fig. 5L).

Effects of CuONPs exposure on the TXNIP-related signaling pathway in COPD mice

The COPD group showed a significantly increased expression of TXNIP and IL-1β in the lung tissue compared with the NC group (Fig. 6A–C). Moreover, CuONPs exposure in COPD mice significantly elevated TXNIP and IL-1β expression in the lung tissue compared to the COPD group. Additionally, Western blotting demonstrated a markedly increased expression of TXNI, IL-1β, NLRP3, and caspase-1 in CuONPs-exposed COPD mice compared with the COPD group (Fig. 6D–H). All these effects occurred in a dose-dependent manner.

Effects of TXNIP overexpression on the pathophysiology of CuONPs exposure in COPD mice

We identified the TXNIP overexpression using the AAV system according to previously described method [31] (Supplementary Figure S4). The TXNIP-overexpressed COPD group showed significantly increased inflammatory cell count and cytokines compared with the COPD group (Fig. 7A–G). Furthermore, TXNIP overexpression markedly increased inflammatory cell count and cytokines in CuONPs-exposed COPD mice. These responses were consistent with histopathology results. TXNIP overexpression in CuONPs-exposed COPD mice significantly elevated inflammatory cell infiltration and mucus production compared with the CuONPs-exposed COPD group (Fig. 7H–K). Additionally, the expression of 8-OHdG and MDA in the CuONPs-exposed COPD group significantly increased due to TXNIP overexpression, while SOD activity was markedly decreased (Fig. 7L–N). Moreover, TXNIP-overexpressed CuONPs-exposed COPD mice showed significantly elevated IL-1β, NLRP3, and caspase-1 expression compared with their counterparts (Fig. 7O–T).

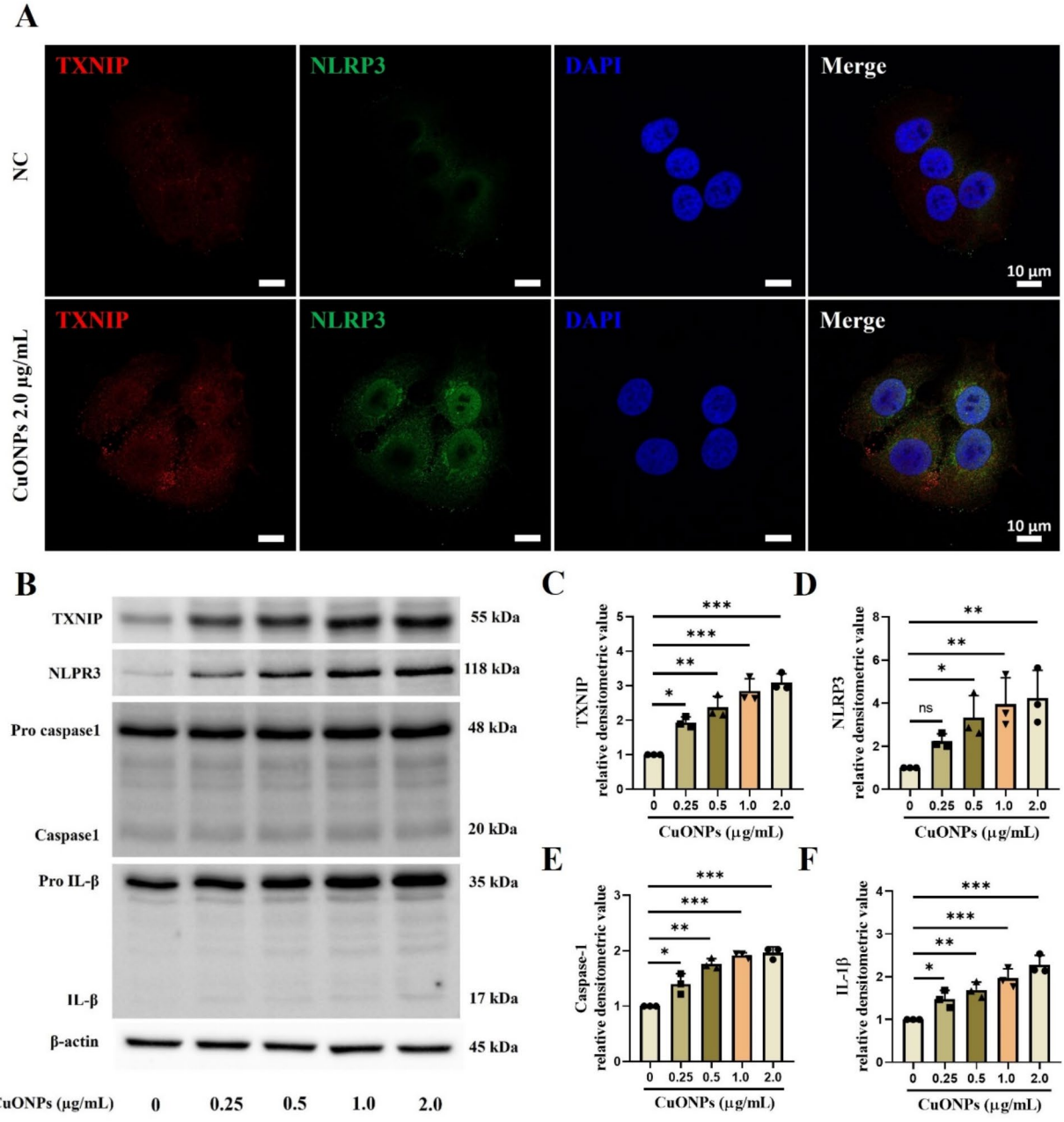

Fig. 3 Pathophysiological alterations of CuONPs-treated NCI-H292 cells. (**A**) TXNIP and NLRP3 expression by double-immunofluorescence stain (Bar = 10 μm). (**B**–**F**) Protein expression and relative densitometric values. Data are indicated as means ± SD ($n = 3$). *, **, *** Significant differences from the control group, $p < 0.05$, $p < 0.01$, and $p < 0.001$, respectively

Effects of TXNIP deletion on the pathophysiology of CuONPs exposure in COPD mice

TXNIP-KO COPD mice showed significantly reduced inflammatory cell counts and cytokines compared with the COPD group (Fig. 8A–G). Furthermore, TXNIP deletion markedly decreased the inflammatory cell count and cytokines in CuONPs-exposed COPD mice. These responses were consistent with histopathology results demonstrating significantly reduced inflammatory cell infiltration and mucus production in CuONPs-exposed COPD mice (Fig. 8H–K). Furthermore, 8-OHdG and MDA expression in the CuONPs-exposed COPD group significantly decreased by TXNIP deletion, whereas SOD activity was markedly reduced (Fig. 8L–N). Moreover, TXNIP-KO CuONPs-exposed COPD mice showed significantly reduced IL-1β, NLRP3, and caspase-1 expression compared with the CuONPs-exposed COPD mice (Fig. 8O–T).

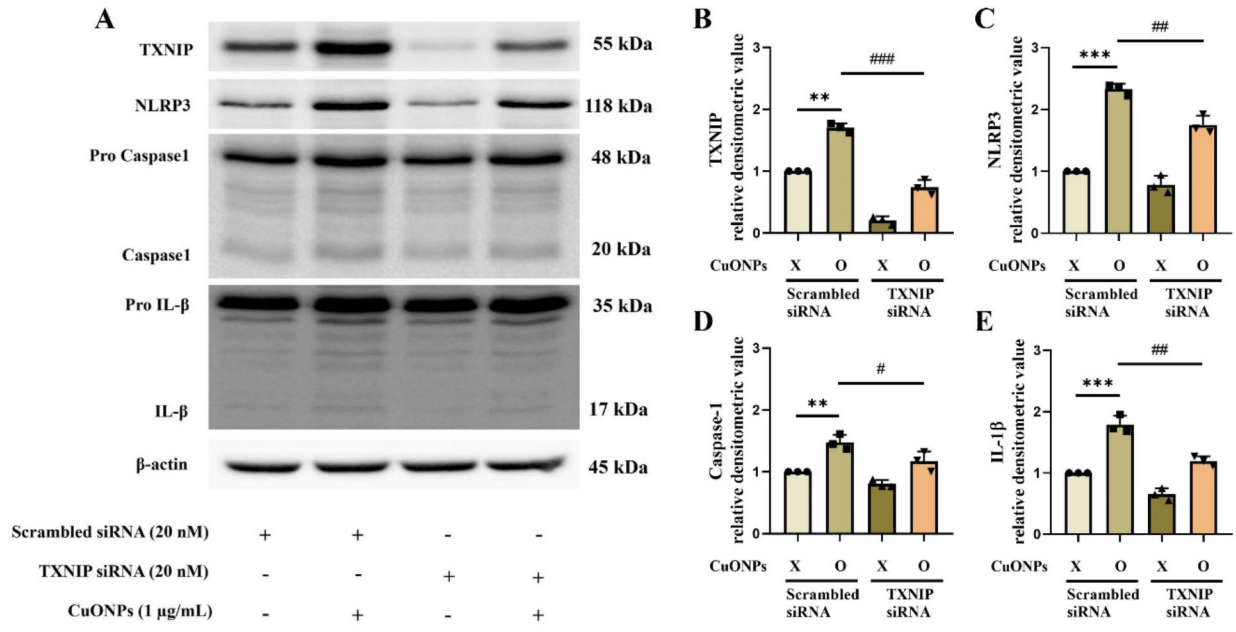

Fig. 4 Effects of downregulation of TXNIP on CuONPs-provoked inflammation in NCI-H292 cells. (**A**–**E**) Protein expression and relative densitometric values. Data are indicated as means ± SD ($n = 3$). **, *** Significant differences from the scrambled siRNA group, $p < 0.01$ and $p < 0.001$, respectively; $^{\#}$, $^{\#\#}$, $^{\#\#\#}$ Significant differences from the scrambled siRNA + CuONPs group, $p < 0.01$, $p < 0.05$, and $p < 0.001$, respectively

Discussion

Currently, nanomaterials are utilized in an array of industries and disciplines due to their unique thermophysical properties and antibacterial activity [2, 5, 32]. With the increasing use of nanomaterials, there is a growing realization of the potential threats they pose to human health. CuONPs, one of the most commonly used nanomaterials, are being employed across various industries, including healthcare [6, 32]. However, CuONPs could be toxic to the respiratory tract since they induce respiratory inflammation via excessive ROS generation [33]. Consequently, various toxicity studies of CuONPs have been conducted, but basic research data on the potential toxicity of CuONPs remains insufficient. Particularly, research on the toxicity mechanisms and their potential to exacerbate underlying diseases is scarce. In this study, we examined the respiratory toxicity of CuONPs and the pathophysiology of CuONPs exposure in COPD using TXNIP-overexpressed and TXNIP-KO mice. CuONPs exposure in normal mice induced inflammatory responses, such as inflammatory cell infiltration, mucus production, and cytokines production, with elevated TNXIP expression. Additionally, CuONPs exposure in COPD mice markedly elevated TXNIP-related signaling with increased various inflammatory indexes. TXNIP-overexpressed CuONPs-exposed COPD mice showed markedly increased COPD-related indexes and expression of IL-1β, caspase-1, and NLRP3 compared with their counterparts. Conversely, in TXNIP-KO CuONPs-exposed mice, these responses were reversed and decreased compared to CuONPs-exposed COPD mice.

Exposure to CuONPs caused respiratory inflammation with elevated inflammatory cell counts and cytokines in a dose-dependent manner, which induced certain alterations in COPD mice. CuONPs exposure in COPD mice markedly increased inflammatory responses with increased oxidative damage, as evidenced by increased levels of 8-OHdG and MDA, and decreased SOD activity. These findings were also observed in a previous study [24, 34]. Exposure to CuONPs induces neutrophilic inflammation of the respiratory tract and aggravates allergic responses in asthma by elevating inflammatory cytokines and oxidative stress [24]. Specifically, the involvement of neutrophils is central to the pathogenesis of COPD. Because neutrophils are associated with the release and production of inflammatory cytokines, ROS and proteinases, increased neutrophilic inflammation accelerates the progression of COPD [28]. Therefore, CuONPs exposure may accelerate the development of COPD. Additionally, we observed increased TXNIP expression in the respiratory tract due to CuONP exposure, which was also detected when exposing COPD mice to CuONPs. Hence, CuONPs exposure–induced alterations in the respiratory tract correlate with TXNIP expression.

TXNIP is an endogenous inhibitor of thioredoxin and is associated with the progression of various disorders, such as myocardial injury, COPD, diabetic kidney disease, and several inflammatory conditions [11, 21, 29,

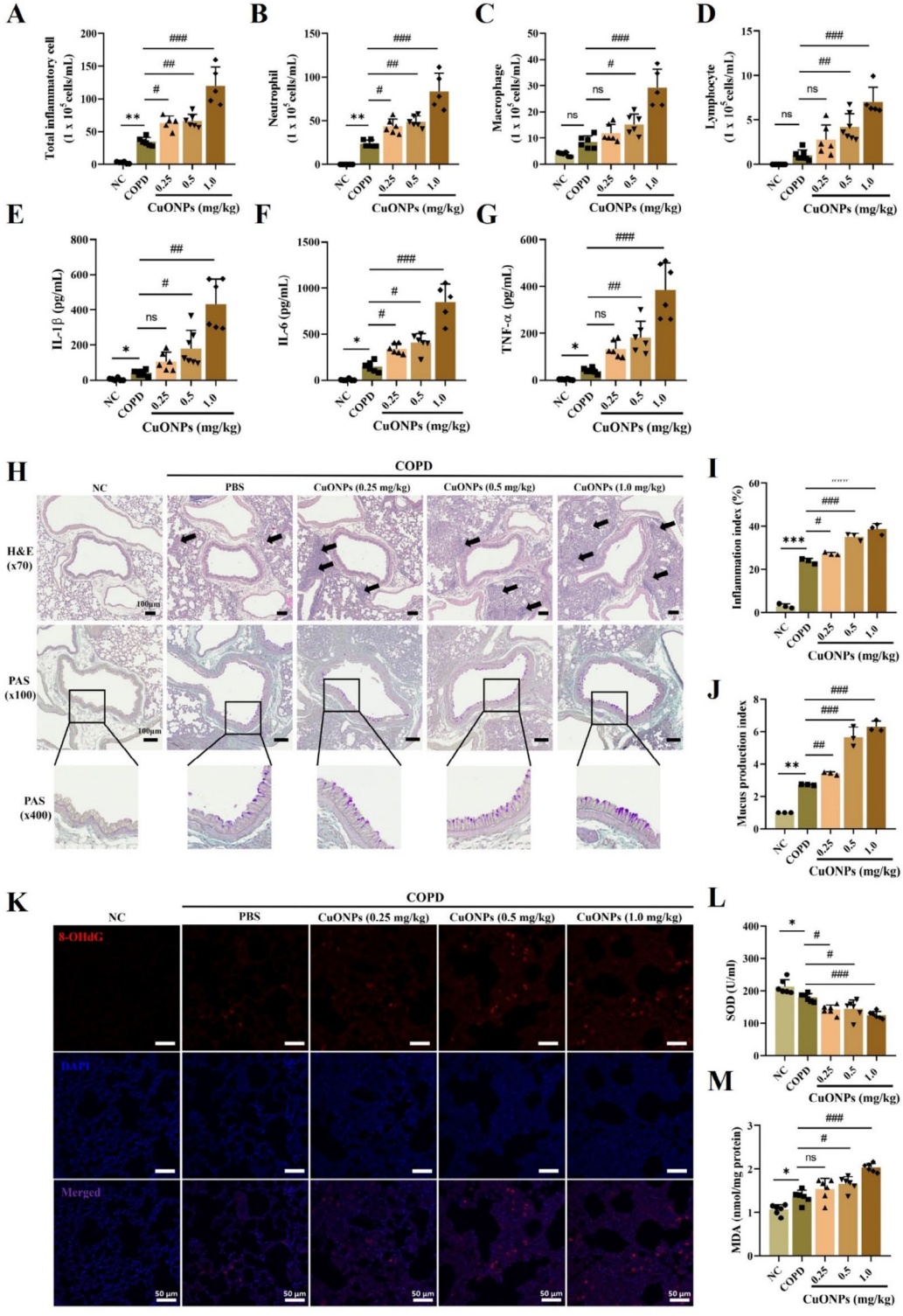

Fig. 5 Effects of CuONPs exposure on the progression of COPD mice. (**A**–**D**) Inflammatory cell counts in BALF. (**E**–**G**) Inflammatory cytokines in BALF. (**H**) Staining with hematoxylin and eosin (× 70, Bar = 100 μm) and periodic acid-schiff (× 100, × 400, Bar = 100 μm) on lung tissue. The black arrows represent inflammatory cell infiltration. (**I** and **J**) Quantitative analysis of the inflammatory infiltration and mucus production, respectively. (**K**) 8-OhdG expression by immunofluorescence stain (Bar = 50 μm). (**L** and **M**) The levels of MDA and the activities of SOD in lung. Data are indicated as means ± SD ($n = 6$). *, **, *** Significant differences from the NC group, $p < 0.05$, $p < 0.01$, and $p < 0.001$, respectively; $^{\#}$, $^{\#\#}$, $^{\#\#\#}$ Significant differences from the COPD group, $p < 0.01$, $p < 0.05$, and $p < 0.001$, respectively

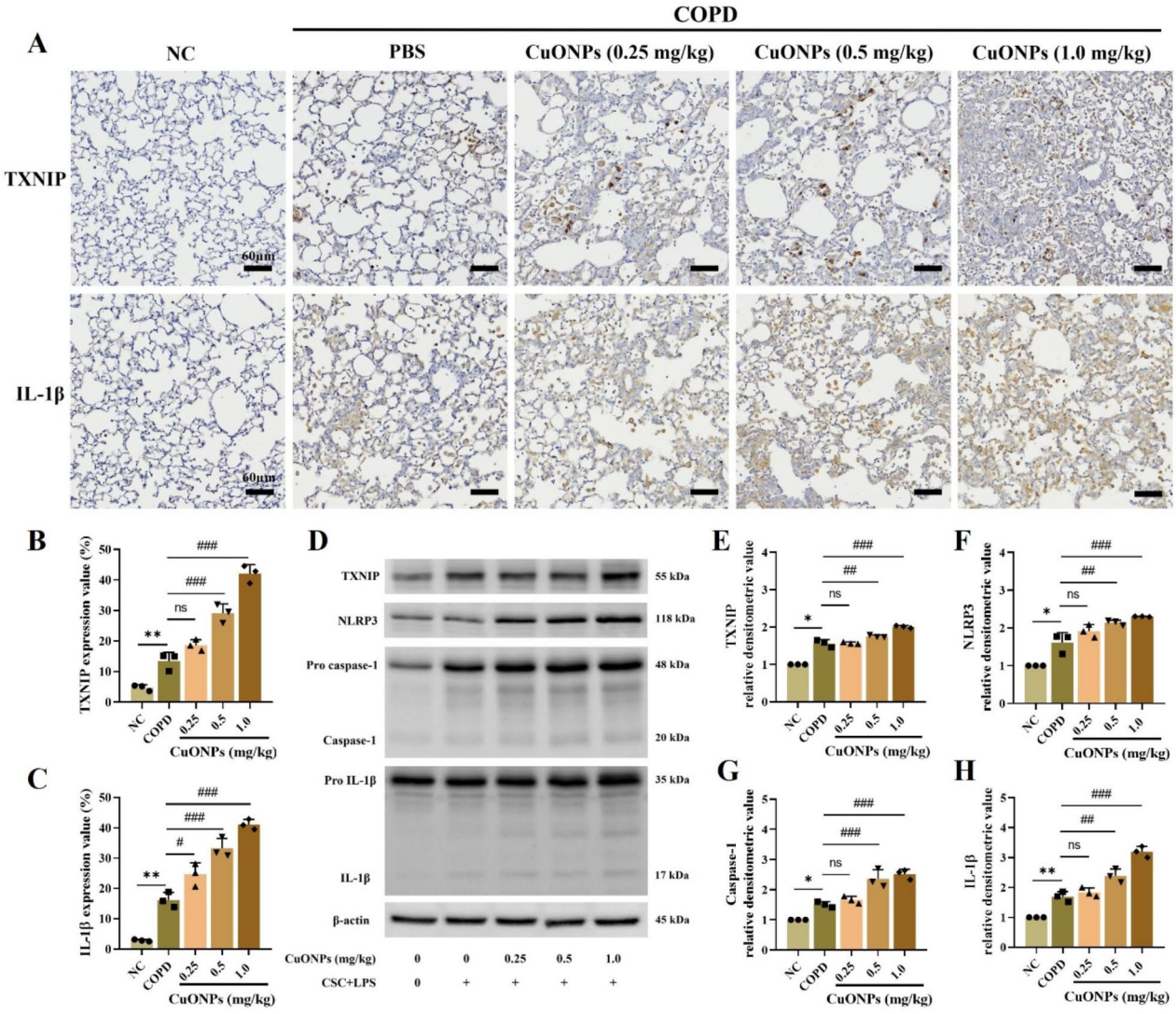

Fig. 6 Effects of CuONPs exposure on TXNIP related signaling pathway in COPD mice. (**A**–**C**) Expression of TXNIP and IL-1β (× 200, Bar = 60 nm) and expression value. (**D**–**H**) Protein expression and relative densitometric values. Data are indicated as means ± SD ($n = 3$). *, ** Significant differences from the NC group, $p < 0.05$ and $p < 0.01$, respectively; $^{\#}$, $^{\#\#}$, $^{\#\#\#}$ Significant differences from the COPD group, $p < 0.01$, $p < 0.05$, and $p < 0.001$, respectively

35, 36]. TXNIP, a possible binding partner of NLRP3 in the yeast two-hybrid system with leucine-rich repeats, is produced from oxidized TRX under oxidative stress and attaches to the NLRP3 inflammasome [16, 37]. This complex activates and releases IL-1β and caspase-1, stimulating inflammatory responses [38]. Particularly, TXNIP activation can be elicited by several stimuli, including smoking and nanomaterials [11, 21, 29]. In previous studies, exposure to cigarette smoke or nanomaterials, including titanium dioxide and silica dioxide, increased ROS and triggered the TXNIP pathway, increasing IL-1β and caspase-1 expression, eventually resulting in an inflammatory response with oxidative stress induction in the respiratory tract. In this study, exposure to CuONPs induced inflammatory responses in the respiratory tract and increased TXNIP expression along with the associated signaling pathway. Additionally, elevated TXNIP expression was detected in COPD mice. Furthermore, exposure to CuONPs in COPD mice caused an even greater increase in TXNIP expression and associated signaling pathway compared with non-exposed COPD mice, thereby accelerating the development of COPD. These results indicate that CuONPs-induced respiratory inflammation and exacerbation of COPD are associated with TXNIP expression.

TXNIP is associated with the progression of ROS-related disorders [16, 39, 40]. TRX serves as a key defender of cells against oxidative stress through its

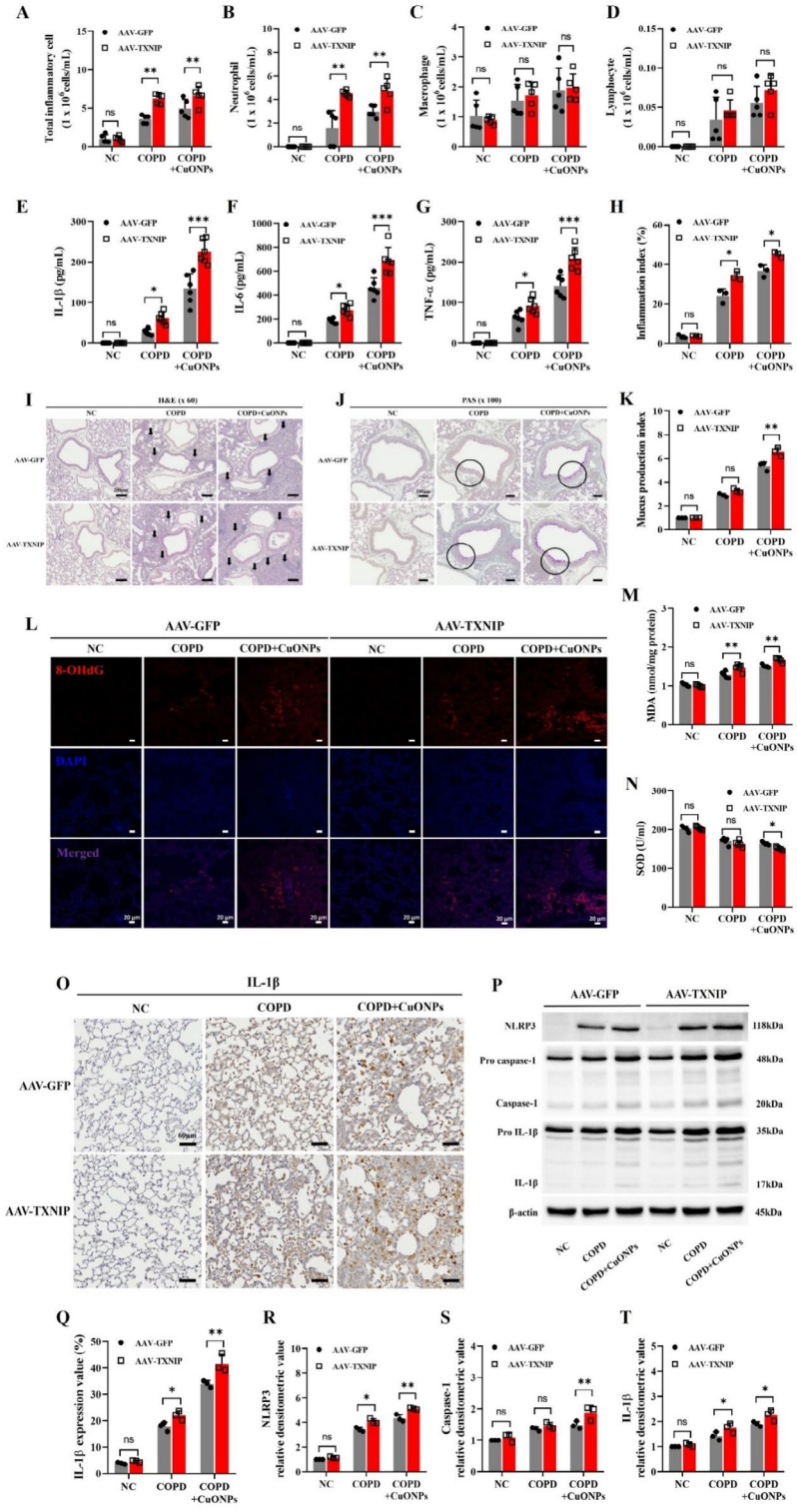

Fig. 7 Effects of TXNIP overexpression on pathophysiological alteration in CuONPs-exposed COPD mice. (**A**–**D**) Inflammatory cell counts in BALF. (**E**–**G**) Inflammatory cytokines in BALF. (**I**) Staining with hematoxylin and eosin (× 60, Bar = 200 μm) on lung tissue. Black arrows represent inflammatory cell infiltration. (**J**) Staining with periodic acid-schiff (× 100, Bar = 100 μm) on lung tissue. (**H** and **K**) Quantitative analysis of the inflammatory infiltration and mucus production, respectively. (**L**) 8-OhdG expression by immunofluorescence stain (Bar = 20 μm). (**M** and **N**) The levels of MDA and the activities of SOD in lung. (**O** and **Q**) Expression of IL-1β (× 200, Bar = 60 nm) and expression value. (**P** and **R**–**T**) Protein expression and relative densitometric values. Data are indicated as means ± SD ($n = 6$; **A**–**G**, $n = 3$; **H**–**T**). Significant differences are shown by the following symbols: $^{*}p < 0.05$, $^{**}p < 0.01$, and $^{***}p < 0.001$

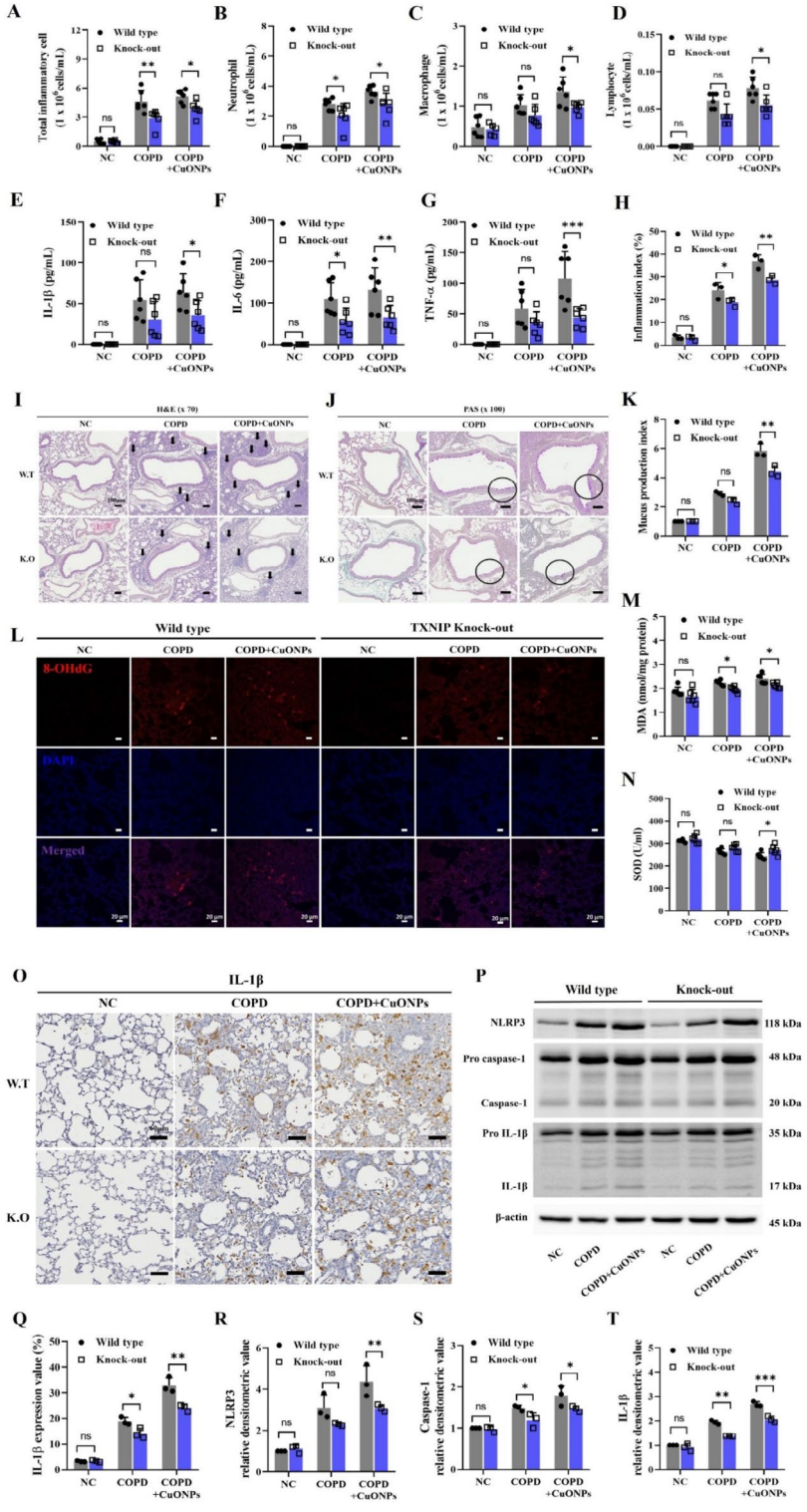

Fig. 8 Effects of TXNIP deletion on the pathophysiological alteration in CuONPs-exposed COPD mice. (**A**–**D**) Inflammatory cell counts in BALF. (**E**–**G**) Inflammatory cytokines in BALF. (**I**) Staining with hematoxylin and eosin (× 70, Bar = 100 μm) on lung tissue. Black arrows represent inflammatory cell infiltration. (**J**) Staining with periodic acid-schiff (× 100, Bar = 100 μm) on lung tissue. (**H** and **K**) Quantitative analysis of the inflammatory infiltration and mucus production, respectively. (**L**) 8-OhdG expression by immunofluorescence stain (Bar = 20 μm). (**M** and **N**) The levels of MDA and the activities of SOD in lung. (**O** and **Q**) Expression of IL-1β (× 200, Bar = 60 nm) and expression value. (**P** and **R**–**T**) Protein expression and relative densitometric values. Data are indicated as means ± SD ($n = 6$; **A**–**G**, $n = 3$; **H**–**T**). Significant differences are shown by the following symbols: $^{*}p < 0.05$, $^{**}p < 0.01$, and $^{***}p < 0.001$

ROS-scavenging activity and inhibition of apoptosis [41, 42]. However, TXNIP covalently binds to and suppresses TRX, stimulating oxidative stress and apoptosis [43]. These alterations are also very important in the pathogenesis of COPD. Excess production of ROS, known as oxidative stress, induces an imbalance between antioxidants and oxidants, increases the production of proinflammatory mediators, and damages cells, accelerating the progression of COPD [44]. Therefore, the modulation of TXNIP expression is an important strategy in controlling COPD [45]. In this study, CuONPs exposure in COPD mice significantly increased oxidative stress and decreased antioxidant enzymes, exacerbating various indicators of COPD. Additionally, increased oxidative stress induced by CuONPs exposure is accompanied by elevated TXNIP expression. Hence, the effects of CuONPs on the respiratory tract might be associated with increased oxidative stress due to elevated TXNIP expression.

Finally, we investigated the role of TXNIP in respiratory toxicity and exacerbation of COPD induced by CuONPs exposure using TXNIP-KO mice and AAV-TXNIP transgenic mice. TXNIP overexpression aggravated respiratory inflammation and increased the NLRP3 signaling and COPD-related markers in COPD mice and CuONPs-exposed COPD mice. Conversely, TXNIP deletion significantly reduced not only the NLRP3 signaling but also respiratory inflammation and oxidative stress in COPD mice and CuONPs-exposed COPD mice. The activated TXNIP-NLRP3 signaling increases caspase-1 and IL-1β expression, stimulating inflammatory responses and oxidative stress with elevated inflammatory cytokines [24, 46]. Thus, CuONPs might induce respiratory inflammation and exacerbate COPD by activating the TXNIP-NLRP3 signaling. Moreover, our findings were supported by previous studies [29, 47–49]. Given the pro-inflammatory and pro-apoptotic effects associated with TXNIP upregulation, targeting this pathway may offer a promising strategy to mitigate the acute effects of nanoparticle exposure and develop therapeutic interventions for managing underlying diseases, such as the use of small molecule inhibitors, RNA interference, or antioxidants to modulate TXNIP activity.

While these results are significant, there are certain limitations that should be acknowledged. Our study primarily focused on the acute exposure effects of CuONPs. Although it did not address the potential impacts of chronic exposure to nanoparticles, data on acute exposure are important for establishing baseline effects and can inform the design of future studies on chronic exposure. We also utilized the NCI-H292 cell line, a human bronchial epithelial cell line derived from non-small cell lung cancer, to investigate the effects of CuONPs exposure. Although this cell line has been widely used in experiments on various lung inflammatory responses, it is important to consider that its response to nanoparticle exposure may differ from that of normal bronchial epithelial cells [50]. Additionally, the direct addition of CuONPs to culture media may not fully replicate the interactions of nanoparticles with airway epithelial cells in real-world scenarios where inhalation is the primary route of exposure. Therefore, experiments using models such as aerosolization or air-liquid interface systems may provide more physiologically relevant data [51]. A novel culture system incorporating normal bronchial epithelial cells could enhance our understanding of the effects of CuONPs exposure.

Conclusion

CuONPs exposure significantly increased inflammatory responses in the respiratory tract, which was correlated with elevated TXNIP-NLRP3 signaling. Moreover, we elucidated the exacerbating effect of CuONPs exposure on the respiratory tract with underlying COPD, as well as related signaling transduction via TXNIP regulation. Therefore, our study provides novel information on target signaling in respiratory toxicity and exacerbation of COPD induced by CuONPs exposure and targeting the TXNIP pathway may represent a promising approach for mitigating the respiratory toxicity associated with CuONPs exposure and developing therapeutic interventions for related diseases.

Supplementary Information

The online version contains supplementary material available at https://doi.org/10.1186/s12989-024-00608-3.

Supplementary Material 1

Acknowledgements

The animal experiment in this study was supported the College of Veterinary Medicine and BK21 FOUR Program, Chonnam National University. The authors would like to thank the researchers at Korea Institute of Toxicology for their technical support.

Author contributions

SHK and JCK mainly designed the study. WIK and SWP performed the experiments. SJL, SHP, and JOL analyzed the experimental results. WIK wrote the paper. DIK, ISS, SHK, and JCK assisted the crucial revision of drafts. All authors read and approved the final manuscript.

Funding

This work was supported by the National Research Foundation of Korea (NRF) grant funded by the Korea Government (MSIT) (NRF-2021R1A2C2011673). This research was also supported by 'regional innovation mega project' program through the Korea Innovation Foundation funded by Ministry of Science and ICT (Project Number: 1711202880).

Data availability

No datasets were generated or analysed during the current study.

Declarations

Ethics approval and consent to participate
This research was approved by the Institutional Animal Care Use Committee (IACUC) of Chonnam National University (CNU IACUC-YB-2021-146).

Consent for publication
Not applicable.

Competing interests
The authors declare no competing interests.

Author details
[1]College of Veterinary Medicine and BK21 FOUR Program, Chonnam National University, Gwangju 61186, Republic of Korea
[2]Herbal Medicine Resources Research Center, Korea Institute of Oriental Medicine, Naju 58245, Republic of Korea
[3]Jeonbuk Branch Institute, Korea Institute of Toxicology, Jeongeup 56212, Republic of Korea

Received: 3 July 2024 / Accepted: 28 October 2024
Published online: 11 November 2024

References

1. Chaudhary RG, Bhusari GS, Tiple AD, Rai AR, Somkuvar SR, Potbhare AK, et al. Metal/metal oxide nanoparticles: toxicity, applications, and future prospects. Curr Pharm Des. 2019;25(37):4013–29.
2. Tulinska J, Mikusova ML, Liskova A, Busova M, Masanova V, Uhnakova I, et al. Copper oxide nanoparticles stimulate the immune response and decrease antioxidant defense in mice after six-week inhalation. Front Immunol. 2022;13:874253.
3. Mendes C, Thirupathi A, Corrêa M, Gu Y, Silveira PCL. The use of metallic nanoparticles in wound healing: new perspectives. Int J Mol Sci. 2022;23(23):15376.
4. Ji H, Guo Z, Wang G, Wang X, Liu H. Effect of ZnO and CuO nanoparticles on the growth, nutrient absorption, and potential health risk of the seasonal vegetable Medicago polymorpha L. PeerJ. 2022;10:e14038.
5. Fu Q, Li W, Kruis FE. Highly conductive copper films prepared by multilayer sintering of nanoparticles synthesized via arc discharge. Nanotechnology. 2023;34(22).
6. Gosens I, Costa PM, Olsson M, Stone V, Costa AL, Brunelli A, et al. Pulmonary toxicity and gene expression changes after short-term inhalation exposure to surface-modified copper oxide nanoparticles. NanoImpact. 2021;22:100313.
7. Pietrofesa RA, Park K, Mishra OP, Johnson-McDaniel D, Myerson JW, Shuvaev VV, et al. Copper oxide nanoparticle-induced acute inflammatory response and injury in murine lung is ameliorated by synthetic secoisolariciresinol diglucoside (LGM2605). Int J Mol Sci. 2021;22(17):9477.
8. Mitra S, Anand U, Ghorai M, Vellingiri B, Jha NK, Behl T, et al. Unravelling the therapeutic potential of botanicals against chronic obstructive pulmonary disease (COPD): molecular insights and future perspectives. Front Pharmacol. 2022;13:824132.
9. Kim JH, Kim JW, Kim CY, Jeong JS, Ko JW, Kim TW. Green tea extract ameliorates macrophage-driven emphysematous lesions in chronic obstructive pulmonary disease induced by cigarette smoke condensate. Phytother Res. 2023;37(4):1366–76.
10. Park SW, Lee AY, Lim JO, Lee SJ, Kim WI, Yang YG, et al. Loranthus tanakae Franch. & Sav. Suppresses inflammatory response in cigarette smoke condensate exposed bronchial epithelial cells and mice. Antioxid (Basel). 2022;11(10):1885.
11. Mahalanobish S, Dutta S, Saha S, Sil PC. Melatonin induced suppression of ER stress and mitochondrial dysfunction inhibited NLRP3 inflammasome activation in COPD mice. Food Chem Toxicol. 2020;144:111588.
12. Wang L, Pelgrim CE, Peralta Marzal LN, Korver S, van Ark I, Leusink-Muis T, et al. Changes in intestinal homeostasis and immunity in a cigarette smoke- and LPS-induced murine model for COPD: the lung-gut axis. Am J Physiol Lung Cell Mol Physiol. 2022;323(3):L266–80.
13. Ni L, Chuang CC, Zuo L. Fine particulate matter in acute exacerbation of COPD. Front Physiol. 2015;6:294.
14. Fan X, Dong T, Yan K, Ci X, Peng L. PM2.5 increases susceptibility to acute exacerbation of COPD via NOX4/Nrf2 redox imbalance-mediated mitophagy. Redox Biol. 2023;59:102587.
15. Mohamed IN, Sarhan NR, Eladl MA, El-Remessy AB, El-Sherbiny M. Deletion of Thioredoxin-interacting protein ameliorates high fat diet-induced non-alcoholic steatohepatitis through modulation of toll-like receptor 2-NLRP3-inflammasome axis: histological and immunohistochemical study. Acta Histochem. 2018;120(3):242–54.
16. Pan M, Zhang F, Qu K, Liu C, Zhang J. TXNIP: a double-edged sword in disease and therapeutic outlook. Oxid Med Cell Longev. 2022;2022:7805115.
17. Choi EH, Park SJ. TXNIP: a key protein in the cellular stress response pathway and a potential therapeutic target. Exp Mol Med. 2023;55(7):1348–56.
18. Zhou R, Tardivel A, Thorens B, Choi I, Tschopp J. Thioredoxin-interacting protein links oxidative stress to inflammasome activation. Nat Immunol. 2010;11(2):136–40.
19. Kelley N, Jeltema D, Duan Y, He Y. The NLRP3 inflammasome: an overview of mechanisms of activation and regulation. Int J Mol Sci. 2019;20(13):3328.
20. Bai R, Lang Y, Shao J, Deng Y, Refuhati R, Cui L. The role of NLRP3 inflammasome in cerebrovascular diseases pathology and possible therapeutic targets. ASN Neuro. 2021;13:17590914211018100.
21. Lim JO, Lee SJ, Kim WI, Pak SW, Kim JC, Kim JS, et al. Melatonin alleviates silica nanoparticle-induced lung inflammation via thioredoxin-interacting protein downregulation. Antioxid (Basel). 2021;10(11):1765.
22. Reddy KD, Oliver BGG. Sexual dimorphism in chronic respiratory diseases. Cell Biosci. 2023;13(1):47.
23. Lim JO, Kim WI, Lee SJ, Pak SW, Cho YK, Kim JC, et al. The involvement of PDE4 in the protective effects of melatonin on cigarette-smoke-induced chronic obstructive pulmonary disease. Molecules. 2021;26(21):6588.
24. Park JW, Lee IC, Shin NR, Jeon CM, Kwon OK, Ko JW, et al. Copper oxide nanoparticles aggravate airway inflammation and mucus production in asthmatic mice via MAPK signaling. Nanotoxicology. 2016;10(4):445–52.
25. Areecheewakul S, Adamcakova-Dodd A, Haque E, Jing X, Meyerholz DK, O'Shaughnessy PT, et al. Time course of pulmonary inflammation and trace element biodistribution during and after sub-acute inhalation exposure to copper oxide nanoparticles in a murine model. Part Fibre Toxicol. 2022;19(1):40.
26. Jeong YJ, Jeon H, Kim EJ, Ryu HY, Song KS, Kang SC. Evaluation of the acute, sub-chronic and chronic oral toxicity, genetic toxicity, and safety of a Lomens-P0. Toxicol Res. 2022;38(1):69–90.
27. Seo HS, Kim JH, Kim SH, Park MK, Seong NW, Kang GH, et al. Toxicity of a 90-day repeated oral dose of a collagen peptide derived from skate (Raja Kenojei) skin: a rat model study. Toxicol Res. 2023;39(3):383–98.
28. Shin IS, Shin NR, Park JW, Jeon CM, Hong JM, Kwon OK, et al. Melatonin attenuates neutrophil inflammation and mucus secretion in cigarette smoke-induced chronic obstructive pulmonary diseases via the suppression of Erk-Sp1 signaling. J Pineal Res. 2015;58(1):50–60.
29. Lim JO, Lee SJ, Kim WI, Pak SW, Moon C, Shin IS, et al. Titanium dioxide nanoparticles exacerbate allergic airway inflammation via TXNIP upregulation in a mouse model of asthma. Int J Mol Sci. 2021;22(18):9924.
30. Lim JO, Kim WI, Pak SW, Lee SJ, Park SH, Shin IS, et al. Toll-like receptor 4 is a key regulator of asthma exacerbation caused by aluminum oxide nanoparticles via regulation of NF-κB phosphorylation. J Hazard Mater. 2023;448:130884.
31. Yang MS, Park MJ, Lee J, Oh B, Kang KW, Kim Y, et al. Non-invasive administration of AAV to target lung parenchymal cells and develop SARS-CoV-2-susceptible mice. Mol Ther. 2022;30(5):1994–2004.
32. Jain A, Ranjan S, Dasgupta N, Ramalingam C. Nanomaterials in food and agriculture: an overview on their safety concerns and regulatory issues. Crit Rev Food Sci Nutr. 2018;58(2):297–317.
33. Lai X, Zhao H, Zhang Y, Guo K, Xu Y, Chen S, et al. Intranasal delivery of copper oxide nanoparticles induces pulmonary toxicity and fibrosis in C57BL/6 mice. Sci Rep. 2018;8(1):4499.
34. Kumar R, Nagesha DK. Size-dependent study of pulmonary responses to nano-sized iron and copper oxide nanoparticles. Methods Mol Biol. 2013;1028:247–64.
35. Gao C, Wang R, Li B, Guo Y, Yin T, Xia Y, et al. TXNIP/Redd1 signalling and excessive autophagy: a novel mechanism of myocardial ischaemia/reperfusion injury in mice. Cardiovasc Res. 2020;116(3):645–57.
36. Schneider MR, Zettler S, Rathkolb B, Dahlhoff M. TXNIP overexpression in mice enhances streptozotocin-induced diabetes severity. Mol Cell Endocrinol. 2023;565:111885.

37. Kaimul AM, Nakamura H, Masutani H, Yodoi J. Thioredoxin and thioredoxin-binding protein-2 in cancer and metabolic syndrome. Free Radic Biol Med. 2007;43(6):861–8.
38. Zhang Y, Wang J, Wang X, Li A, Lei Z, Li D, et al. TXNIP aggravates cardiac fibrosis and dysfunction after myocardial infarction in mice by enhancing the TGFB1/Smad3 pathway and promoting NLRP3 inflammasome activation. Acta Biochim Biophys Sin (Shanghai). 2023;55(12):1950–60.
39. Zhou J, Chng WJ. Roles of thioredoxin binding protein (TXNIP) in oxidative stress, apoptosis and cancer. Mitochondrion. 2013;13(3):163–9.
40. García-Hernández B, Morán J. Txnip expression promotes JNK-mediated neuronal death in response to reactive oxygen species. Front Mol Neurosci. 2023;16:1210962.
41. Tsubaki H, Tooyama I, Walker DG. Thioredoxin-interacting protein (TXNIP) with focus on brain and neurodegenerative diseases. Int J Mol Sci. 2020;21(24):9357.
42. Ha JH, Lee BW, Yi DH, Lee SJ, Kim WI, Pak SW, et al. Particulate matter-mediated oxidative stress induces airway inflammation and pulmonary dysfunction through TXNIP/NF-κB and modulation of the SIRT1-mediated p53 and TGF-β/Smad3 pathways in mice. Food Chem Toxicol. 2024;183:114201.
43. Zhao Y, Chen Y, Liu Z, Zhou L, Huang J, Luo X, et al. TXNIP knockdown protects rats against bupivacaine-induced spinal neurotoxicity via the inhibition of oxidative stress and apoptosis. Free Radic Biol Med. 2024;219:1–16.
44. Sunnetcioglu A, Alp HH, Sertogullarından B, Balaharoglu R, Gunbatar H. Evaluation of oxidative damage and antioxidant mechanisms in COPD, lung cancer, and obstructive sleep apnea syndrome. Respir Care. 2016;61(2):205–11.
45. Kansal H, Chopra V, Garg K, Sharma S. Role of thioredoxin in chronic obstructive pulmonary disease (COPD): a promising future target. Respir Res. 2023;24(1):295.
46. Zou L, Cheng G, Xu C, Liu H, Wang Y, Li N, et al. Copper nanoparticles induce oxidative stress via the heme oxygenase 1 signaling pathway in vitro studies. Int J Nanomed. 2021;16:1565–73.
47. Wang K, Ning X, Qin C, Wang J, Yan W, Zhou X, et al. Respiratory exposure to copper oxide particles causes multiple organ injuries via oxidative stress in a rat model. Int J Nanomed. 2022;17:4481–96.
48. Sajjad H, Sajjad A, Haya RT, Khan MM, Zia M. Copper oxide nanoparticles: in vitro and in vivo toxicity, mechanisms of action and factors influencing their toxicology. Comp Biochem Physiol C Toxicol Pharmacol. 2023;271:109682.
49. Duan S, Wang H, Gao Y, Wang X, Lyu L, Wang Y. Oral intake of titanium dioxide nanoparticles affect the course and prognosis of ulcerative colitis in mice: involvement of the ROS-TXNIP-NLRP3 inflammasome pathway. Part Fibre Toxicol. 2023;20(1):24.
50. Newland N, Richter A. Agents associated with lung inflammation induce similar responses in NCI-H292 lung epithelial cells. Toxicol Vitro. 2008;22(7):1782–8.
51. Offer S, Di Bucchianico S, Czech H, Pardo M, Pantzke J, Bisig C, et al. The chemical composition of secondary organic aerosols regulates transcriptomic and metabolomic signaling in an epithelial-endothelial in vitro coculture. Part Fibre Toxicol. 2024;21(1):38.

Publisher's note